Chemical Engineering & Processing: Process Intensification 136 (2019) 36–43

Contents lists available at ScienceDirect

Chemical Engineering & Processing: Process Intensification

journal homepage: www.elsevier.com/locate/cep

Preparation of fluorescent waterborne polyurethane nanodispersion by high-gravity miniemulsion polymerization for multifunctional applications

Haotian Liu[a,b], Tingting Hu[b], Dan Wang[a,*], Jie Shi[a,b], Jianjun Zhang[a], Jie-Xin Wang[a,b], Yuan Pu[a,*], Jian-Feng Chen[a,b]

[a] Research Centre of the Ministry of Education for High Gravity Engineering and Technology, Beijing University of Chemical Technology, Beijing, 100029, China
[b] Beijing Aerospace Propulsion Institute, Beijing, 100076, China

ARTICLE INFO

Keywords:
Waterborne polyurethane nanodispersion
High-gravity technology
Process intensification
Fluorescent nanoparticles
AIEgens

ABSTRACT

Polymer encapsulated fluorescent nanoparticles have found many applications in bioimaging, fluorescent gels and inks. However, their translation into the practical products has been slow because it is still difficult to produce nanoparticles that are consistent “batch-to-batch” for scale-up. Herein, we develop a high-gravity miniemulsion polymerization route for fluorescent waterborne polyurethane (PU) by using rotating packed bed (RPB) reactor for process intensification. In optimized conditions, the PU nanoparticles obtained exhibited an average size of 137 nm with narrow size distribution. Dispersion stability of the PU nanodispersions was investigated and no significant sediments or aggregates were observed for up to one month. The 1,1,2,3,4,5-hexaphenylsilole dyes, a kind of typical aggregation-induced emission luminogens (AIEgens), could be in situ loaded in PU nanoparticles, forming fluorescent nanodispersions of AIEgens@PU in aqueous solution. The preliminary applications of AIEgens@PU nanodispersion for in vitro fluorescent labeling of cells, transparent fluorescent films and anti-counterfeit printing inks were demonstrated. This study demonstrated that the newly developed high-gravity miniemulsion polymerization method provides an effective route to waterborne PU nanodispersion for multifunctional applications.

1. Introduction

Aqueous polymeric nanodispersions have recently attracted increasing attention for coatings, adhesives and biomedical vehicles, due to of their unique properties such as easy fabrication, volatile organic compounds (VOC) free and outstanding performance [1]. Of particular importance is the aqueous polyurethane (PU) nanodispersion, which has shown significant advantages in terms of good biocompatibility, potential biodegradability and facile surface functionalization for biomedical applications [2–5]. The miniemulsion polymerization process is among the most attractive methods for the production of high quality aqueous PU nanodispersion with uniform particle size distribution [6]. In a typical miniemulsion polymerization method, small droplets containing organic solvent, monomers and organic emitters are directly formed via mechanical stress and then act as confined nanoreactors [7]. Following the in situ polymerization in the droplets, in the most frequent situation, each nanoemulsion droplet forms one nanoparticle. In other words, the polymeric nanoparticles formed as one to one copy of the droplets in the solution [8,9]. One of the key issues to control the particle size distribution is to achieve homogeneous micromixing at molecular scale before the micellar nucleation [10]. To date, the general methods to perform miniemulsion in aqueous solution were based on the high shear of high-speed dispersion, high-pressure homogenizers and ultrasonication in conversional stirred reactors (STR) [11]. However, the effective production of PU nanoparticles with controllable size distribution has been limited by the low mass transfer efficiency and relatively long micromixing characteristic time of STR [12,13]. In addition, complete control of the reaction parameters and batch-to-batch replicability are hard to achieve in traditional batch type reactors for those fast reactions, especially when large volumes of solution are involved [14]. Therefore, process intensification based on various types of reactor or technology is highly needed in for continuous production of aqueous polymeric nanodispersions.

The rotating packed bed (RPB) reactor is a typical apparatus to mimic the high-gravity environment for process intensification in chemical industry [15]. In the RPB reactor, the micro-mixing and mass transfer efficiency of the fluid can be enhanced by 1–3 orders of magnitude compared with that in conversional STR [16–18]. In the last

* Corresponding authors at: Research Centre of the Ministry of Education for High Gravity Engineering and Technology, Beijing University of Chemical Technology, Beijing, 100029, China.
E-mail addresses: wangdan@mail.buct.edu.cn (D. Wang), puyuan@mail.buct.edu.cn (Y. Pu).

https://doi.org/10.1016/j.cep.2018.12.012
Received 20 October 2018; Received in revised form 23 December 2018; Accepted 27 December 2018
Available online 28 December 2018
0255-2701/

decades, the high-gravity technology has been demonstrated as an efficient tool for scalable synthesis of both organic nanoparticles and inorganic nanocrystals via nanoprecipitation [19,20]. A few studies showed the advantages of high-gravity technique for the preparation of emulsions, in which none of chemical reaction was involved [16,21,22]. However, the process intensification for the preparation of polymeric nanodispersions by high-gravity RPB has not been reported to the best of our knowledge.

In this work, we developed a high-gravity miniemulsion polymerization approach for the synthesis of aqueous waterborne PU nanodispersion based on the use of RPB reactor. The influence of high-gravity levels (G = 100 *g*, 200 *g*, 300 *g* and 400 *g*) on the products of PU nanodispersion was investigated. PU nanoparticles with average size of 137 nm and narrow size distribution were obtained and no significant sediments or aggregates in the aqueous solution were observed for up to one month. DFT simulation was performed to obtain the knowledge for the chemical reaction process during the polymerization. Fluorescent nanoparticles doped with aggregation-induced emission luminogens (AIEgens) were synthesized and their preliminary applications for in vitro fluorescent labeling of cells, transparent fluorescent films and anti-counterfeit printing inks were demonstrated. The high-gravity miniemulsion polymerization provides a new platform for preparation of aqueous PU nanodispersion in a facile and controllable manner, which is promising for large scale production in industry.

2. Experimental section

2.1. Materials

Isophorone dissocyanate (IPDI), 1,2-pentanediol (1,2-PD), 1,12-dodecanediol, sodium dodecyl sulfate (SDS), ethylene glycol, glycerol, poly(acrylic acid), dimethyl sulfoxide (DMSO) and ditin butyl dilaurate (DBTDL) were purchased from Aladdin Industrial Corporation. 1,1,2,3,4,5-Hexaphenylsilole (HPS), phosphate buffered saline (PBS), 3-(4,5-dimethylthiazol-2-yl)-2,5-diphenyltetrazolium bromide (MTT) and paraformaldehyde are purchased from Sigma-Aldrich. All the chemicals were used without any additional purification unless specifically mentioned. The human breast cancer cells (MDA-MB-231 cells) line was obtained from American Type Culture Collection (ATCC). Deionized water obatained by a laboratory water purification system was used for all experiments.

2.2. Synthesis of PU nanodispersion

The synthesis of PU nanoparticles was conducted by two-step process, which was composed of pre-polymerization process and miniemulsion polymerization process (Fig. 1). Briefly, 4.0 *g* of IPDI, 2.1 *g* of 1,2-PD and 4 μL of DBTDL were stirred together in a 20 mL beaker at 15 °C for 10 min to synthesis PU oligomers (solution A). Meanwhile, 100 mg of SDS was dissolved in 100 mL of water, forming homogeneous solution (solution B). For the miniemulsion polymerization, solution A and B were pumped into a RPB reactor via two inlets at liquid flow rates of 50 mL/min. Four different high gravity levels (G = 100 *g*, 200 *g*, 300 *g* and 400 *g*) were adopted in our experiments to study the influence of the experimental parameters on the product of PU nanodispersions. The temperature of the reaction system was controlled at 20 °C during the miniemulsion process and the microemulsion was then stirred at 70 °C for 2 h, allowing complete polymerization of the reactants to form nanoparticles. The nanoparticles were purified by washing and centrifugal separation three times to remove the surfactants. The core component of RPB reactor is a rotator with 2.5 cm thick stainless packing, and the detailed setup information on the RPB reactor can be found in previous reports [18].

For the preparation of PU encapsulated fluorescent nanoparticles containing AIEgens (AIEgens@PU), 10 mg of HPS was added during the synthesis of prepolymer (solution A). Other experimental parameters were the same as for the synthesis of PU nanodispersion.

2.3. Characterization

The polymer molecular weights were determined by gel permeation chromatography (GPC, 1515GPC, Waters, America) analysis. The Fourier transform infrared (FTIR) spectra were carried out using a PerkinElmer Spectrum GX FTIR spectroscopy system in the range of 400-4000 cm^{-1}. The ^{13}C- nuclear magnetic resonance (NMR) spectra were recorded using Bruker AVANCE III HD NMR spectroscopy, in $CDCl_3$, using tetramethylsilane (TMS). The particle sizes were measured by dynamic light scattering (DLS) at 5 mg/mL. The morphologies of the PU nanoparticles were observed by a Hitachi HT7700 transmission electron microscopy (TEM) at an accelerating voltage of 100 kV and a JEOL JSM-7800 F scanning electron microscope (SEM) at an accelerating voltage of 10.0 kV. The visible transmittance spectra were using a Shimadzu UV-2600 Spectrometer. The fluorescence spectra were recorded using an Edinburgh Instruments FS5 Fluorescence Spectrometer.

2.4. Computational details

All calculations in this work are done in the $DMol^3$ code based on the spin-unrestricted DFT method [23,24]. We used the generalized gradient approximation (GGA) with the PBE functional [25], in combination with the double numerical basis sets with polarization functions (DNP). For more accurate calculation of long range force, TS method for DFT-D correction were used. We set the convergence thresholds for energy, force, and displacement to be 2.0×10^{-5} Ha, 0.004 Ha/Å, and 0.005 Å, respectively. The smearing of electronic occupations was set to be 0.005 Ha. The search protocol was set to be linear synchronous transit (Complete LST/QST) method, in order to obtain the minimum energy pathway (MEP).We computed the vibrational frequencies of each structure along the MEP at the same level, to confirm that a transition state has one and only imaginary frequency. The charge is set after the introduction of ionic catalyst. For other parameters, the default settings are taken.

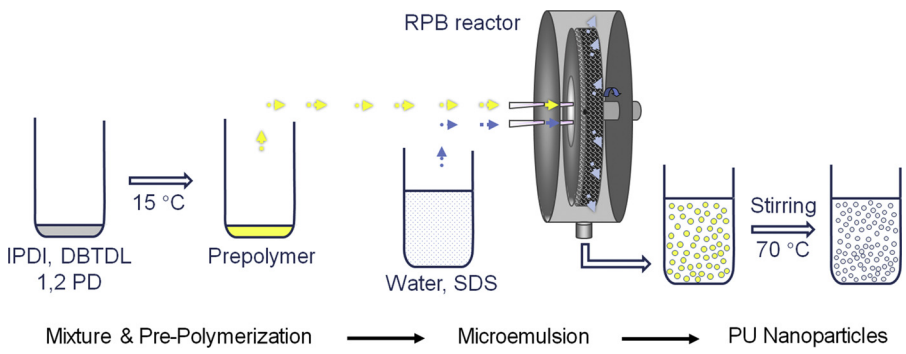

Fig. 1. Schematic of the process flow for the synthesis of PU nanoparticles via high-gravity miniemulsion polymerization.

2.5. Cytotoxicity of AIEgens@PU nanodispersion

The in vitro cytotoxicity of AIEgens@PU against MDA-MB-231 cells was assessed by MTT assay. Typically, 100 μL MDA-MB-231 cells were seeded in 96-well plates at a density of 4 × 10 [4] cells/mL. After 12 h incubation at 37 °C in 5% CO_2 atmosphere, the cells were exposed to a series of doses of AIEgens@PU nanoparticles. After 24 h, the sample wells were washed once with 100 μL 1 × PBS buffer, and 20 μL MTT solution (5 mg/mL 1 × PBS) in culture medium were added into each sample well. The MTT-medium solution was removed after 4 h incubation in the incubator, and 100 μL DMSO was then added into each well. The plate was gently shaken for 10 min in the incubator to dissolve all of the precipitates formed. The absorbance at 570 nm was then monitored by a Tecan GENios Microplate Reader.

2.6. AIEgens@PU nanodispersion for in vitro fluorescence imaging of cells

The MDA-MB-231 cells were cultured in the incubator at 37 °C in 5% CO_2 atmosphere. The AIEgens@PU nanoparticles were added to the chamber (100 μg/mL). After incubation for 4 h, the cells were washed twice times with 1 × PBS buffer. The cells were fixed with 4% paraformaldehyde for 20 min and were further washed twice with 1 × PBS buffer. The cells were then imaged by confocal laser scanning microscopy (CLSM) (TCS SP8, Leica, Germany) upon excitation at 405 nm laser and the fluorescent signals were collected at above 480 nm.

2.7. AIEgens@PU nanodispersion for fluorescent patterning

200 mg AIEgens@PU powder, 4 mL water, 4 mL ethylene glycol, 2 mL glycerol and 0.5 mL poly(acrylic acid) were stirred together in a 20 mL beaker. The mixture was homogeneity by 1 min ultrasonic treatment.

3. Results and discussion

The main reaction and side reaction during the synthesis of waterborne polyurethane nanodispersion were shown in Fig. 2. The main reaction involves the addition polymerization between IPDI and 1,2-PD, forming oligomers containing isocyanate group. However, in the presence of water, the side reaction occurs, which lead to by-products such as urea and biuret.

The DFT simulations were used to understand the formation process of dimers during the prepolymerization. The prepolymerization reaction is the process in which hydroxyl groups lose protons and isocyanate groups acquire protons. Based on the above, the reactivity of hydroxyl groups with respect to nucleophilic attack affects the reaction selectivity. The nucleophilic Fukui field showed that the alpha hydroxyl of 1,2-PD have the stronger reactivity than the beta hydroxyl of 1,2-PD (Fig. 3b). The greater values of the yellow cloud part in the picture indicate a greater susceptibility to attack. The Fukui field calculation results corresponds to the LUMO value of 1,2-PD which also showed that the alpha hydroxyl have the stronger reactivity (Fig. 3a). However, there is no significant difference in the HOMO of the two isocyanate groups of IPDI (Fig. 3a). The above calculation results indicated that the prepolymerization reaction occurred between alpha hydroxyl of 1,2-PD and isocyanate group of IPDI. The EHOMO and ELUMO have been showed in the figure. The free energy profile of reactants, transition states, and product for IPDI + 1,2PD → PU dimer showed that the reaction is more difficult to spontaneously (Fig. 3d). The optimized geometries and key chemical bond lengths of reactants, transition states, and product for the reaction process between alpha hydroxyl of 1,2-PD and isocyanate group of IPDI were showed in the Fig. 3c. Sn^{2+} is often used as a catalyst in the reaction to accelerate the reaction rate and increase the selectivity of the reaction. The free energy profile of reactants, transition states, and intermediates for catalysis showed that the catalyst greatly reduces the reaction energy barrier. An intermediate with 5-membered heterocyclic structure was found in the calculation process, which was more stabled than the intermediate with 6-membered heterocyclic structure of the previous reaction mechanism (Fig. 3f). Two kinds of the intermediate structure in the catalytic reaction process have been showed in Fig. 3e.

The ^{13}C NMR spectra in Fig. 4a shows experimental evidence for the theory analysis. The peaks of alpha carbon and beta carbon could be found at 66.71 and 72.08 ppm in the ^{13}C NMR spectrum of 1,2-PD. The chemical groups in the IPDI are hard to be determined since IPDI isomers are mixture of cis isomers and trans-isomers. In the ^{13}C NMR spectra of PU oligomers, several new peaks at 69.19, 70.18, 156.03 and 157.35 ppm emerged and no significant chemical shift of beta carbon was found, indicating the reaction occurred between beta hydroxyl of 1,2-PD and isocyanate group of IPDI. Fig. 4b shows the FTIR spectra of PU nanoparticles, in which the characteristic peak at 2275–2250 cm^{-1} ($\upsilon_{-N=C=O}$) from isocyanate groups disappeared, and the characteristic peaks of PU nanoparticles at about 1702 cm^{-1} ($\upsilon_{C=O}$), 1551 cm^{-1} (δ_{N-H}) and 1310 cm^{-1} (υ_{C-N}) emerged. The characteristic peak at 3342 (υ_{OH}) from water was also observed, which was due to the incompletely dehydration under low temperature. These results also proved

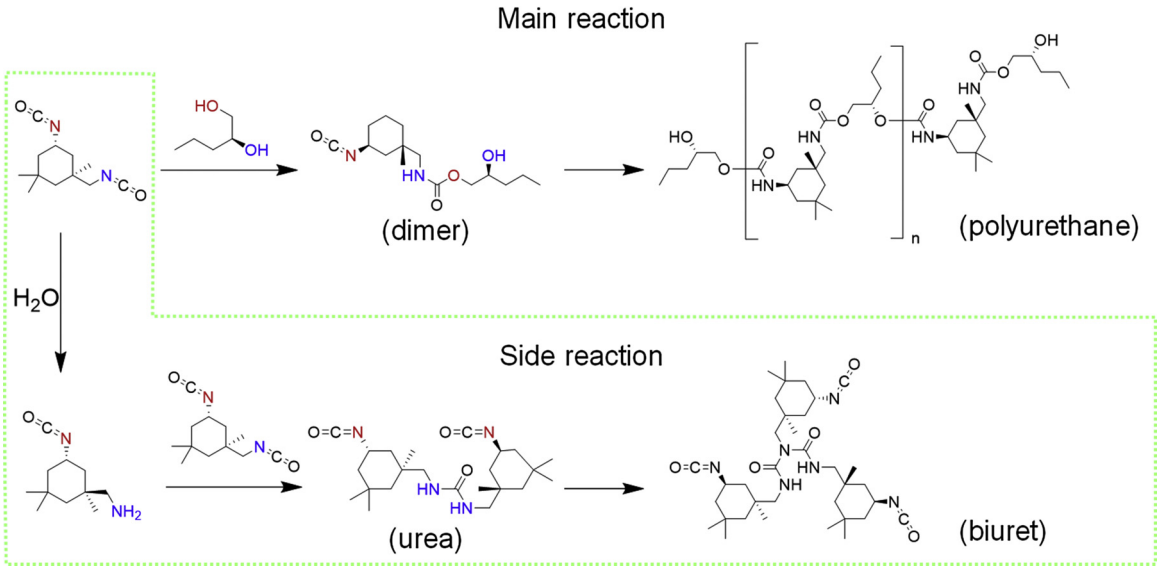

Fig. 2. The main reaction and side reaction among IPDI, 1,2-PD and water.

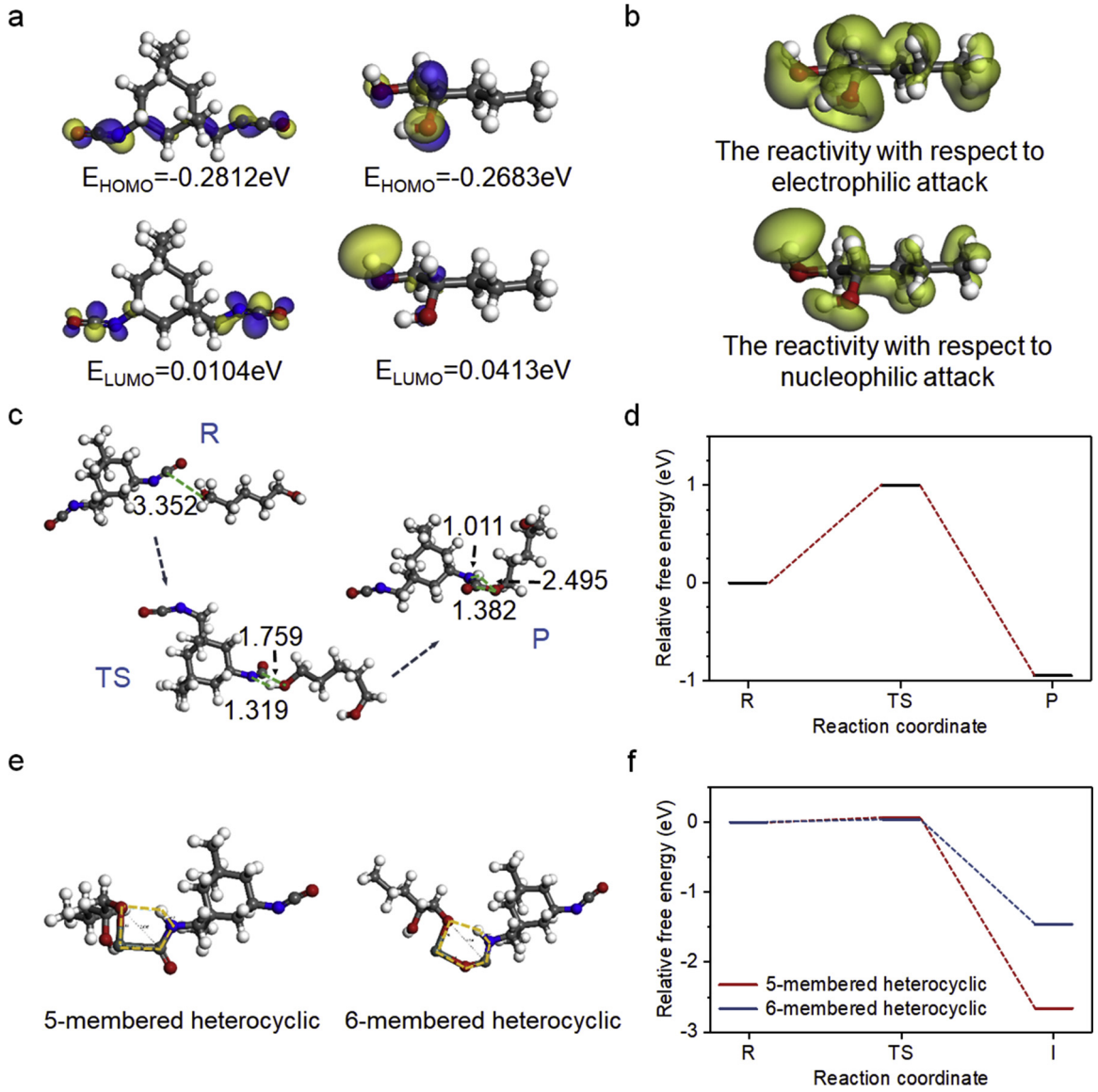

Fig. 3. (a) HOMO and LUMO for IPDI and 1,2-PD. The calculations were performed at the B3LYP hybrid functional; (b) Fukui field, greater values indicate a greater susceptibility to attack. The isovalue for surfaces is 0.03; (c) the optimized geometries and key chemical bond lengths of reactants, transition states, and product for the reaction process between alpha hydroxyl of 1,2-PD and isocyanate group of IPDI; (d) free energy profile of reactants, transition states, and product for IPDI + 1,2PD → PU dimer; (e) the intermediate structure of the catalytic reaction process; (f) free energy profile of reactants, transition states, and intermediates for IPDI + 1,2PD → PU dimer with Sn^{2+}.

evidences for the conversion of IPDI. The polymer molecular weights of PU nanoparticles determined by GPC was Mw = 2069 Da.

Fig. 5a presents a typical SEM image of the dry powder of PU nanoparticles via RPB technique, which exhibited spherical shape with diameters of around 100 nm. The agglomeration interaction of the particles was attributed to the dry process for the preparation of the powder for SEM observation. Fig. 5b presents a typical SEM image of the dry powder of PU nanoparticles via traditional stirred-tank reactor (STR) route, which exhibited agglomerate and accidented. A series digital photos of the PU nanodispersion synthesized via RPB technique and STR route with solid content of 50 mg/mL indicating the highly dispersing of PU nanoparticles in aqueous solution (Fig. 5c–h). No significant sedimentation of solid particles synthesized via RPB technique from the suspension were observed after stored at 30 °C for 5 days (Fig. 5h). Conversely, the sedimentation of PU particles synthesized via STR route from the suspension were observed in a day (Fig. 5d).

In order to investigate the influence of high-gravity level of the RPB reactor for the preparation of PU nanodispersion, the products obtained at $G = 100\,g$, $200\,g$, $300\,g$ and $400\,g$ were analyzed by DLS measurements. Fig. 6a shows the size distribution of the particles obtained at four conditions and Fig. 6b presents the average diameters of the PU nanoparticles, which were 161.3, 137.8, 135.4, and 158.1 nm for the high gravity level of $100\,g$, $200\,g$, $300\,g$ and $400\,g$, respectively. These results indicate that the high gravity level of the RPB has influenced the size of the particle. The samples also showed low polydispersity index (PDI) values (Fig. 6c), demonstrating the highly dispensability of PU nanoparticles in aqueous solution. It was also noted that, the enhancement of high gravity level of RPB could lead to smaller PU particles (i.e. from $100\,g$ to $200\,g$). However, when the high gravity level was higher than $300\,g$, the average size of the final PU nanoparticles became larger as the increasing of the high gravity level. This is because once the high gravity level beyond the optimized value, the residence time of the mixture in the RPB reactor will be too short to form the uniform and stable microemulsion droplets and the effectiveness of the process intensification by is reduced. Therefore, confirming of optimized experimental conditions for the high-gravity miniemulsion

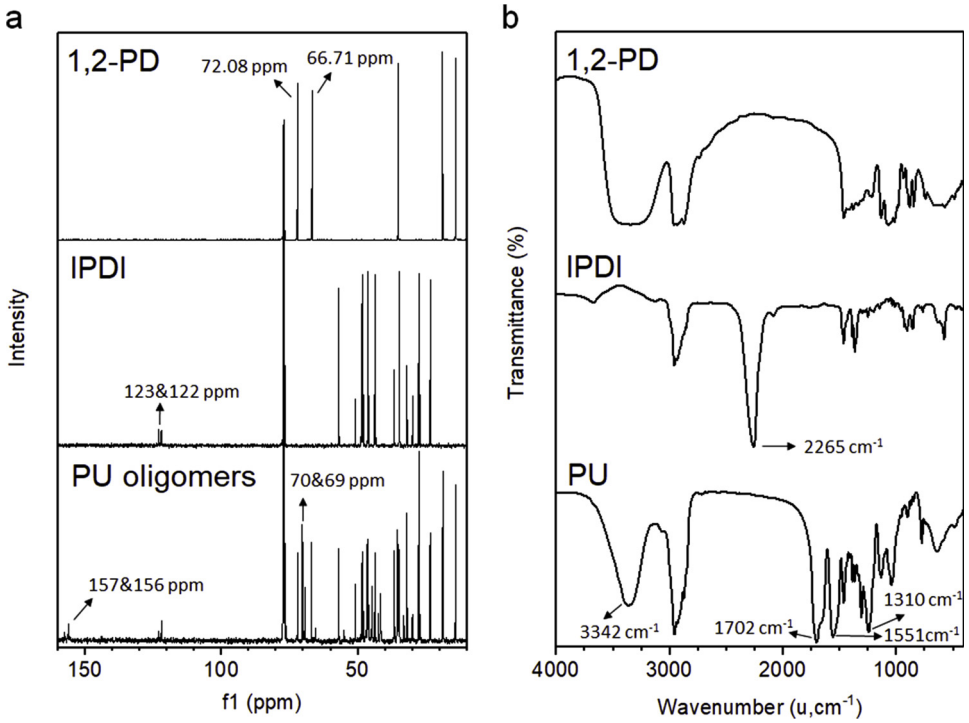

Fig. 4. (a) ^{13}C NMR spectra of 1,2-PD, IPDI and PU oligomers; (b) FTIR spectra of 1,2-PD, IPDI and PU nanoparticles obtained by high-gravity miniemulsion polymerization process.

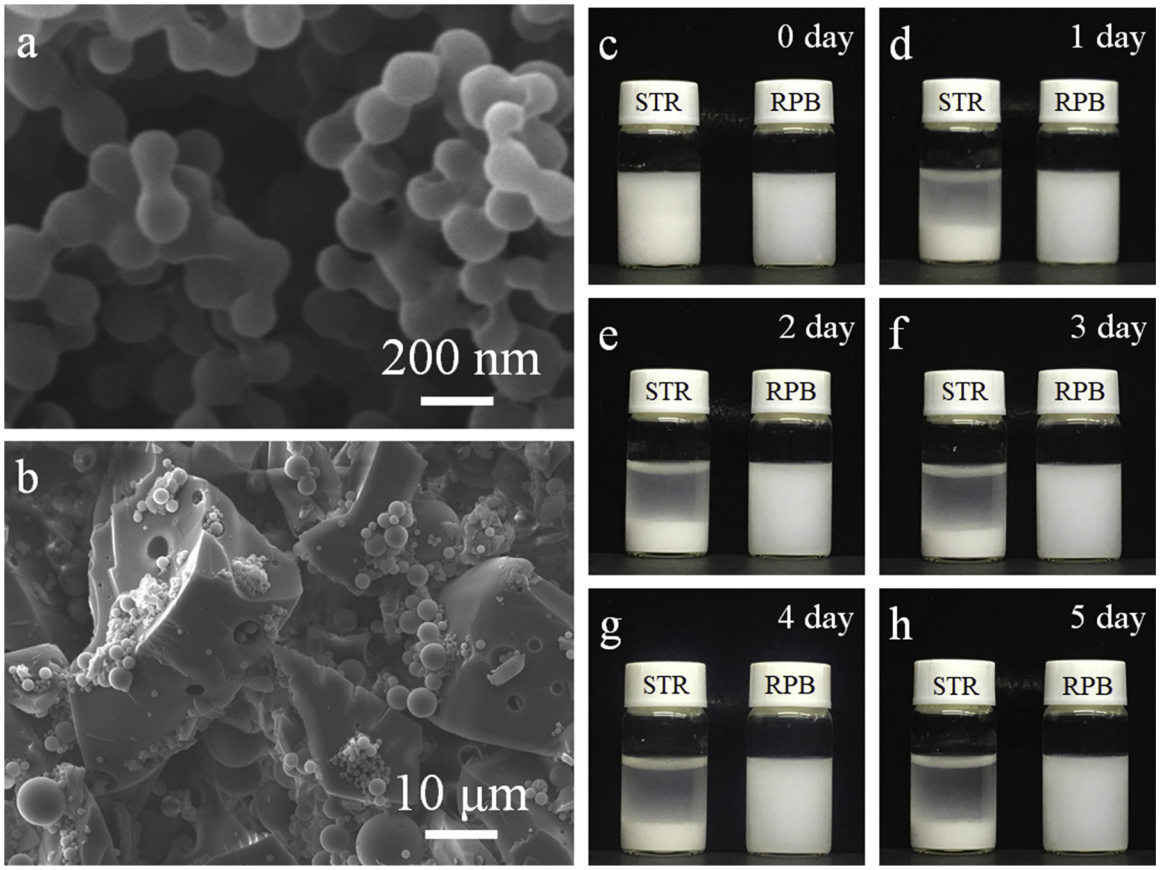

Fig. 5. (a–b) The typical SEM images of PU nanoparticles prepared with (b) and without (a) RPB reactor, respectively; (c–h) a series typical digital photo of fresh PU nanodispersion prepared via STR and RPB with content of 50 mg/mL, the dispersion were stored at 30 °C for 1–5 days.

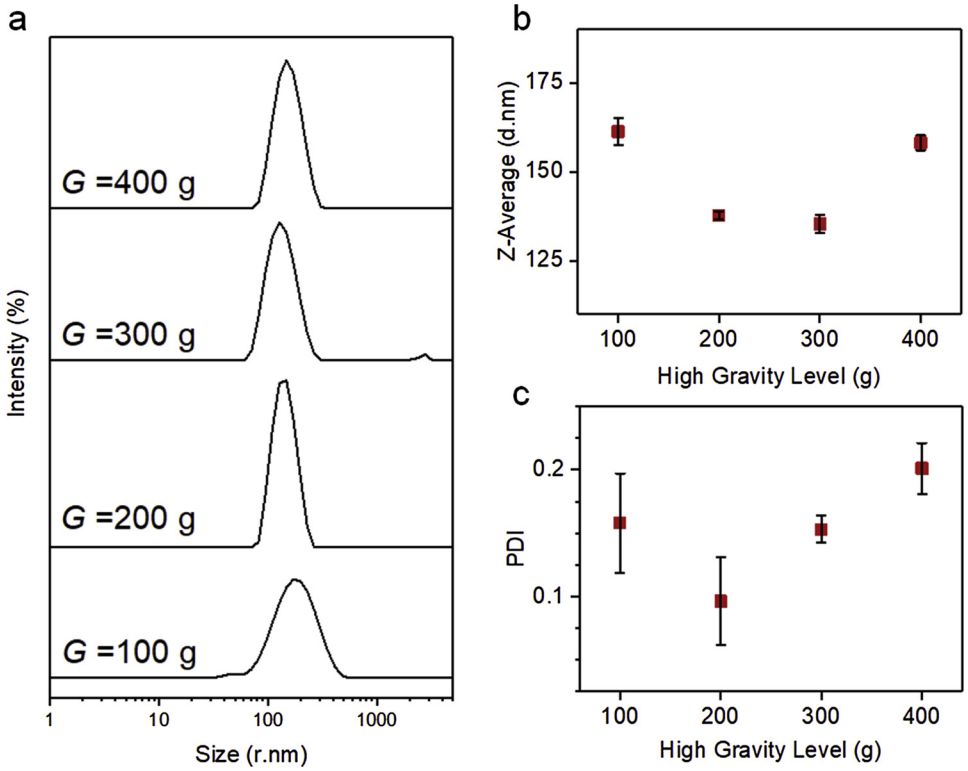

Fig. 6. (a) The particle sizes distribution of PU nanoparticles obtained at our different high gravity levels; (b) the Z-average size and (c) polydispersity index of PU nanoparticles obtained at different high gravity levels.

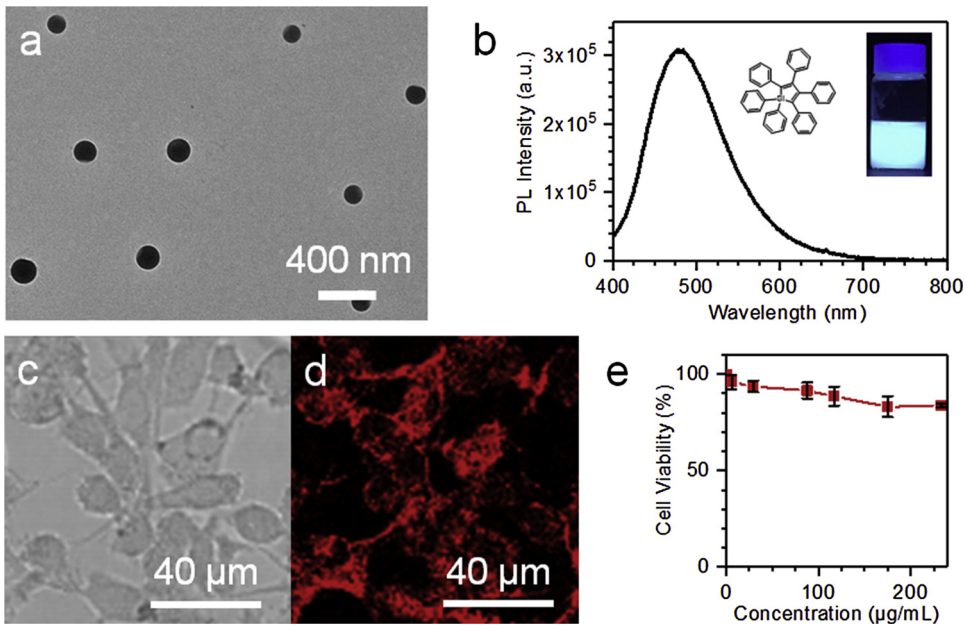

Fig. 7. (a) A typical TEM image of the AIEgens@PU nanoparticles; (b) PL spectra of AIEgens@PU nanoparticles (Inset: the molecular structure of HPS and a digital photo of the AIEgens@PU nanodispersion under UV light); (c) bright field image and (d) fluorescent image of the MDA-MB-231 Cells incubated with AIEgens@PU nanoparticles for 4 h at 37 °C; (e) cell viability of MDA-MB-231 cells incubated with different doses of AIEgens@PU nanoparticles for 24 h at 37 °C in 5% CO_2 atmosphere by MTT assay.

polymerization of aqueous polymeric nanodispersions are critical for specific applications. In our experiments, we identify the high gravity level of 200 *g* as the optimal parameter for the synthesis of PU nanodispersion.

Due to the unique properties of PU such as easy functionalization, biocompatibility and biodegradability, the PU nanoparticles are considered as the ideal vehicle in bio-medical fields. To promote the multifunctional applications of PU nanodispersion, fluorescent nanoparticles doped with AIEgens were prepared. As a demonstration, we employ the in-situ polymerization method to load the fluorescent dyes with aggregation-induced emission (AIEgens) into the PU nanoparticles, forming highly dispersed fluorescent nanodispersions of AIEgens@PU. The HPS molecules were dissolved in the IPDI before the mixing of the precursor and were in situ loaded into the PU nanoparticles during the miniemulsion polymerization process. The TEM photograph in Fig. 6a shows that the microscopic morphology of AIEgens@PU nanoparticles is similar to the PU nanoparticles, but the particle size has a small increase. The PL spectra shows that the emission peak of AIEgens@PU nanoparticles dispersion is at 480 nm (Fig. 6b, λ_{ex} = 370 nm), exhibiting bright blue light under UV light.

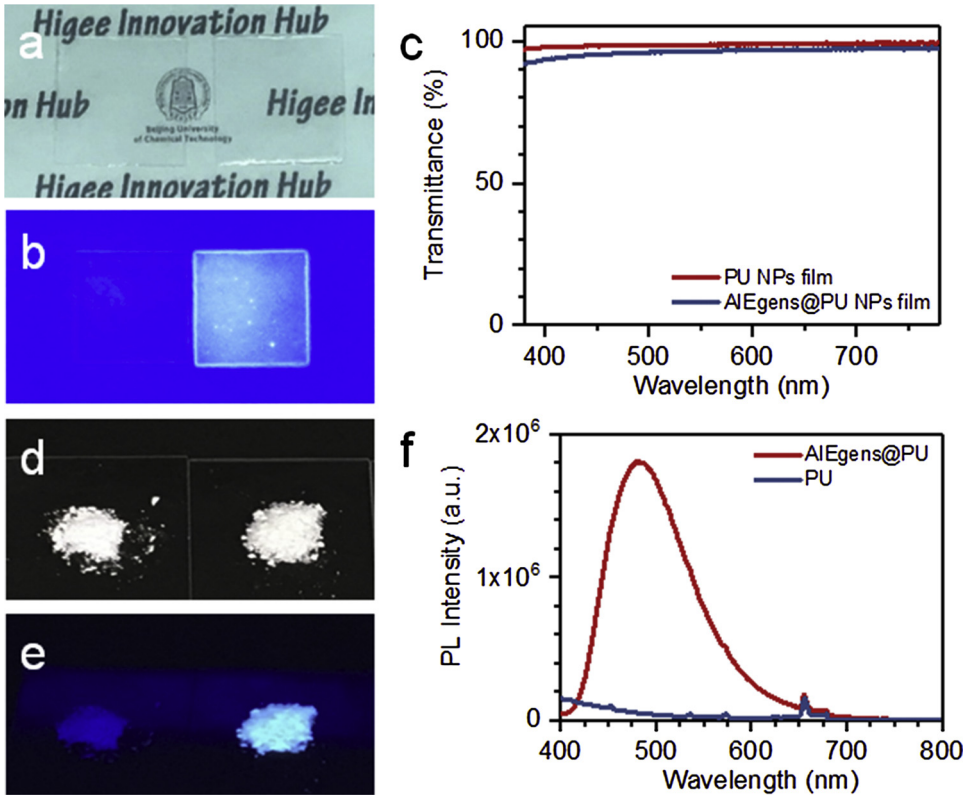

Fig. 8. (a–b) digital photos of PU NPs and AIEgens@PU NPs film under daylight (a) and under UV light (b), respectively; (c) visible transmittance spectra of PU nanoparticles film and AIEgens@PU nanoparticles film; (d–e) digital photos of PU nanoparticles and AIEgens@PU nanoparticles powder under daylight (d) and under UV light (e), respectively; (f) PL spectra of PU nanoparticles and AIEgens@PU nanoparticles powder.

Fig. 7c and d show the images of MDA-MB-231 cells incubated with 100 μg/mL AIEgens@PU nanoparticles for 4 h. According to the bright-field images, the morphologies of cells kept very well, indicating the AIEgens@PU nanoparticles did not cause significant toxicity to the cells. The fluorescence images illustrated that the fluorescence of AIEgens@PU nanoparticles could be clearly observed from the cytoplasm of the cells. These results demonstrated the efficient uptake of AIEgens@PU nanoparticles by MDA-MB-231 cells. Fig. 7e shows the relative cell viability for MDA-MB-231 cells treated with different concentrations of the AIEgens@PU nanoparticles for 4 h. No significant cytotoxicity of cells was caused by the AIEgens@PU even at high concentration of 250 μg/mL, making them promising candidates for cellular imaging agents and drug carriers in biomedical research.

The unique optical properties and good dispersibility of AIEgens@PU nanoparticles in aqueous solution make them ideal precursors for transparent luminescent films and luminescent inks. Fig. 8a shows two transparent films made by mixing the waterborne polyurethane latex with PU nanoparticles and AIEgens@PU nanoparticles, respectively. Both films were highly transparent and were indistinguishable from each other under daylight (Fig. 8a). The visible transmittance spectra of the films showed they have the similar high transparency (Fig. 8c). However, under the irradiation of 365 nm UV light, the AIEgens/PU hybrid film exhibited bright blue emission while no emission was observed from the pure PU film (Fig. 8b), suggesting the promising application of the AIEgens@PU nanodispersion for anti-counterfeiting applications. Furthermore, the AIEgens@PU powder was prepared by centrifugation. The PU powder and AIEgens@PU powder cannot be distinguished by optical photographs taken in daylight (Fig. 8d). Nevertheless, the AIEgens@PU powder emits bright blue emission under UV light (Fig. 8e) with an emission peak at 480 nm (Fig. 8f). The AIEgens@PU powder were added to an ink (4 mL water, 4 mL ethylene glycol, 2 mL glycerol and 0.5 mL poly(acrylic acid)), forming a homogeneous mixture (Fig. 9a) and emitting visually distinguishable blue fluorescence under UV light (Fig. 9b). As demonstrations, we used the prepared anti-counterfeiting ink to write and print on white non-

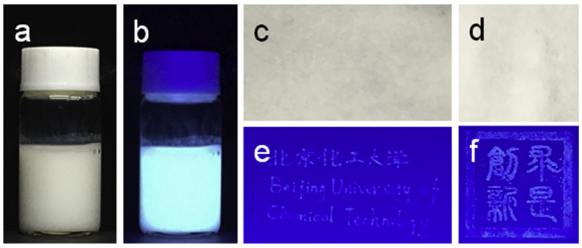

Fig. 9. (a–b) digital photos of the AIEgens@PU-containing ink under daylight (a) and under UV light (b), respectively; (c–f) digital photos of the presswork written or printed using AIEgens@PU-containing ink under daylight (c&d) and under UV light (e&f), respectively.

fluorescent paper. The written and printed content cannot be observed in daylight (Fig. 9c, d). The content can be clearly distinguished under ultraviolet light (Fig. 9e, f), demonstrating that the AIEgens@PU patterns adhered well to commercially available papers. These results suggest that the AIEgens@PU nanodispersion are promising for use in solid-state fluorescent sensing and anti-fake labeling.

4. Conclusion

In summary, we develop a high-gravity miniemulsion polymerization route for synthesis of aqueous PU nanodispersion. The use of high-gravity RPB reactor for process intensification could avoid the side reaction in a larger degree during emulsification process. A combination of theoretical calculations and experiments was carried out on the prepolymerization process in the two-step process. The result showed that the prepolymerization reaction occurred between alpha hydroxyl of 1,2-PD and isocyanate group of IPDI. In optimized conditions, the PU nanoparticles obtained exhibited an average size of 137 nm with narrow size distribution and good dispersiblity. As an ideal vehicle, AIEgens@PU nanoparticles were synthesized as the demonstration of the PU nanoparticles functionalization. The preliminary applications of

AIEgens@PU nanodispersion for in vitro fluorescent labeling of cells, transparent fluorescent films and anti-counterfeit printing inks were demonstrated. This work represents a new strategy for the design and development of waterborne PU for multifunctional applications.

Notes

The authors declare no competing financial interest.

Acknowledgment

We are grateful for financial support from National Key R & D Program of China (2017YFB0404405/2017YFB0404400).

References

[1] N.G. Engelis, A. Anastasaki, G. Nurumbetov, N.P. Truong, V. Nikolaou, A. Shegiwal, M.R. Whittaker, T.P. Davis, D.M. Haddleton, Sequence-controlled methacrylic multiblock copolymers via sulfur-free RAFT emulsion polymerization, Nat. Chem. 9 (2017) 171–178.
[2] T. Wang, D. Chen, Synthesis and properties of self-healing waterborne polyurethanes containing disulfide bonds in the main chain, J. Mater. Sci. 52 (2017) 197–207.
[3] L. Hu, P. Jiang, P. Zhang, G. Bian, S. Sheng, M. Huang, Y. Bao, J. Xia, Amine-graphene oxide/waterborne polyurethane nanocomposites: effects of different amine modifiers on physical properties, J. Mater. Sci. 51 (2016) 8296–8309.
[4] S. Sartori, V. Chiono, C. Tonda-Turo, C. Mattu, C. Gianluca, Biomimetic polyurethanes in nano and regenerative medicine, J. Mater. Chem. B Mater. Biol. Med. 2 (2014) 5128–5144.
[5] H.W. Engels, H.G. Pirkl, R. Albers, R.W. Albach, J. Krause, A. Hoffmann, H. Casselmann, J. Dormish, Polyurethanes: versatile materials and sustainable problem solvers for today's challenges, Angew. Chem. Int. Ed. 52 (2013) 9422–9441.
[6] D. Crespy, K. Landfester, Miniemulsion polymerization as a versatile tool for the synthesis of functionalized polymers, Beilstein J. Org. Chem. 6 (2010) 1132–1148.
[7] H. Wang, L. Wang, R. Wang, X. Tian, Novel route to polyaniline nanofibers from miniemulsion polymerization, J. Mater. Sci. 46 (2011) 1049–1052.
[8] Z.H. Farooqi, A. Ijaz, R. Begum, K. Naseem, M. Usman, M. Ajmal, U. Saeed, Synthesis and characterization of inorganic-organic polymer microgels for catalytic reduction of 4-nitroaniline in aqueous medium, Adv. Manuf. Polym. Compos. Sci. 39 (2018) 645–653.
[9] S.H. Zhang, G. Sun, Y.F. He, R.F. Fu, Y.C. Gu, S. Chen, Preparation, characterization, and electrochromic properties of nanocellulose-based polyaniline nanocomposite films, ACS Appl. Mater. Interface 9 (2017) 16426–16434.
[10] D. Wang, J. Qian, W. Qin, A. Qin, B.Z. Tang, S. He, Biocompatible and photostable AIE dots with red emission for in vivo two-photon bioimaging, Sci. Rep. 4 (2014) 4279.
[11] D.J. McClements, Nanoemulsions versus microemulsions: terminology, differences, and similarities, Soft Matter 8 (2012) 1719–1729.
[12] D. Wang, Z. Wang, Q. Zhan, Y. Pu, J.-X. Wang, N.R. Foster, L. Dai, Facile and scalable preparation of fluorescent carbon dots for multifunctional applications, Engineering 3 (2017) 402–408.
[13] Y. Pu, J. Leng, D. Wang, J.-X. Wang, N.R. Foster, J.-F. Chen, Process intensification for scalable synthesis of ytterbium and erbium co-doped sodium yttrium fluoride upconversion nanodispersions, Powder Technol. 340 (2018) 208–216.
[14] Y. Pu, F.H. Cai, D. Wang, J.X. Wang, J.F. Chen, Colloidal synthesis of semiconductor quantum dots toward large scale production: a review, Ind. Eng. Chem. Res. 57 (2018) 1790–1802.
[15] D. Wenzel, A. Gorak, Review and analysis of micromixing in rotating packed beds, Chem. Eng. J. 345 (2018) 492–506.
[16] H. Zhao, L. Shao, J.-F. Chen, High-gravity process intensification technology and application, Chem. Eng. J. 156 (2010) 588–593.
[17] D.P. Rao, A. Bhowal, P.S. Goswami, Process intensification in rotating packed beds (HIGEE): an appraisal, Ind. Eng. Chem. Res. 43 (2004) 1150–1162.
[18] J.-F. Chen, M.Y. Zhou, L. Shao, Y.Y. Wang, J. Yun, N.Y.K. Chew, H.K. Chan, Feasibility of preparing nanodrugs by high-gravity reactive precipitation, Int. J. Pharmaceut. 269 (2004) 267–274.
[19] D.L. Yang, J. Xiao, D. Wang, W.M. Lin, Y. Pu, X.F. Zeng, Y. Le, J.-X. Wang, Controllable preparation of monodisperse silica nanoparticles using internal circulation rotating packed bed for dental restorative composite resin, Ind. Eng. Chem. Res. 57 (2018) 12809–12815.
[20] J.N. Leng, J.Y. Chen, D. Wang, J.X. Wang, Y. Pu, J.-F. Chen, Scalable Preparation of Gd_2O_3:Yb^{3+}/Er^{3+} Upconversion nanophosphors in a high-gravity rotating packed bed reactor for transparent upconversion luminescent films, Ind. Eng. Chem. Res. 56 (2017) 7977–7983.
[21] Y. Li, R.A. Mei, Z.Q. Yang, A facile method for preparation of emulsion using the high gravity technique, J. Colloid Interface Sci. 506 (2017) 120–125.
[22] Y.Z. Liu, W.Z. Jiao, G.S. Qi, Preparation and properties of methanol-diesel oil emulsified fuel under high-gravity environment, Renew. Energy 36 (2011) 1463–1468.
[23] T. Thonhauser, V.R. Cooper, S. Li, A. Puzder, P. Hyldgaard, D.C. Langreth, Van der Waals density functional: self-consistent potential and the nature of the van der Waals bond, Phys. Rev. B 76 (2007) 125112.
[24] M. Dion, H. Rydberg, E. Schroder, D.C. Langreth, B.I. Lundqvist, Van der Waals density functional for general geometries, Phys. Rev. Lett. 92 (2004) 246401.
[25] J.P. Perdew, K. Burke, M. Ernzerhof, Generalized gradient approximation made simple, Phys. Rev. Lett. 77 (1997) 3865–3868.